Cell Host & Microbe, Volume *15*

Supplemental Information

Emergence and Transmission of Arbovirus Evolutionary Intermediates with Epidemic Potential

Kenneth A. Stapleford, Lark L. Coffey, Sreyrath Lay, Antonio V. Bordería, Veasna Duong, Ofer Isakov, Kathryn Rozen-Gagnon, Camilo Arias-Goeta, Hervé Blanc, Stéphanie Beaucourt, Türkan Haliloğlu, Christine Schmitt, Isabelle Bonne, Nir Ben-Tal, Noam Shomron, Anna-Bella Failloux, Philippe Buchy, and Marco Vignuzzi

Supplemental Information

Figure S1, related to Figure 4. A-B, Binding efficiency of viruses in mammalian BHK (**A**) and mosquito C6/36 (**B**) cells. The parental A226V (P), single mutant P-V80I or P-A129V, or the double mutant P-DM viruses were allowed to bind for the indicated times at 4°C, cells were washed extensively with cold PBS followed by the addition of Trizol and bound virus was quantified by qRT-PCR (n=3, mean and S.E.M. are shown, no significant differences observed, two-tailed unpaired t test). **C-D,** pH dependence of GFP-expressing virus entry in BHK (**C**) or C6/36 (**D**) cells at 16h of infection, following treatment with different concentrations of Bafilomycin A1. The percentage of infected cells was determined by GFP-expression (n=3, mean and S.E.M. are shown, no significant differences observed, two-tailed unpaired t test). **E-H,** One-step viral growth kinetics in mammalian BHK (**E,G**) or mosquito C6/36 (**F, H**) cells. Cells were infected at MOI=1 and at indicated times, infectious progeny was assayed by plaque assay (**E**, **F**) and viral RNA levels were quantified by qRT-PCR (**G**, **H**). n=3, mean and S.E.M are shown, no significant differences were observed, two-tailed unpaired t test. **I,** Expression of glycoproteins by parental A226V (P) or P-DM in BHK cells, the presumed identities of the peptides base on molecular weight are indicated.

Figure S2, related to Figure 4. Electron microscopy reveals no significant differences in virus and cell morphology. A,B, Scanning electron microscopy of parental A226V (**A**) and P-DM (**B**) infected C6/36 mosquito cells showing characteristic budding of chikungunya virus. **C,D,** Transmission electron microscopy of parental A226V (**C**) and P-DM (**D**) infected C6/36 cells revealing similar cell morphology, virus morphology and budding (black arrowheads). **E,F,** Transmission

electron microscopy of parental A226V (**E**) and P-DM (**F**) infected human HeLa cells reveal no significant differences in cell morphology and virus morphology and budding (black arrowheads). **G,H,** Negative-stain transmission electron microscopy of purified A226V (**G**) and P-DM (**H**) virion reveal no significant differences in virus morphology.

Figure S3, related to Figure 4B. Importance of positions 80 and 129 for E1 structural dynamics and function. Normal mode analysis of E1 was conducted using the Gaussian Network Model (GNM)(Emekli et al., 2008; Haliloglu et al., 1997) and the X-ray crystal structure of Chikungunya virus particles E1-E2 (PDB code: 2XFB)(Voss et al., 2010). The E1 molecule is presented using dark colors (orange and grey) and E2 with pale colors (yellow and light grey). The second slowest mode, shown here, divides the dimer into three dynamic domains: The left-most domain, marked with orange (E1) and yellow (E2), the central domain, marked with grey (E1) and light grey (E2), and the right-most, marked with orange (E1). Two hinge regions, marked in magenta, connect the dynamic domains. The left hinge includes positions 52, 108, 214 and 236 of E1, and 72, 74, 77, 231 and 317 of E2. The right hinge includes positions 10, 34, 131, 146, 150, 163, 277, 384 and 389 of E1. The fusion and IJ loops on E1 are shown in green and blue, respectively. Positions 80, 129 and 226 of E1 are highlighted in red. **The V80I mutation,** valine 80 is in a cluster of residues that fluctuate in the fastest mode of E1, implying its function importance. The cluster that includes residues 60, 64, 66, 80, 81 and 100-102 could be important for the structural stability of E1 and also for its interactions with other protein molecules. The cluster is in a 'hot region' of the protein, in the vicinity to the fusion (83-98) and ij (218-235) loops. Specifically, residue 60 of the cluster is in

direct contact with residues 84, 86, 93, 94 and 98 of the fusion loop, and residues 80 and 81 of the cluster are in direct contact with residues 221-224 of the ij loop. Both loops undergo conformation changes. At neutral pH a conformation in which the fusion peptide is buried in a pocket in the E2 protein is assumed. However, in the acidic pH of the endosome E1 detaches from E2, and the ij and fusion loops undergo conformational change that exposes the fusion loop, making it prone to interact with the endosome membrane. The cluster could be involved in the control of this key conformational change and the V80I mutation could alter characteristics of the transition (e.g., affect the relative stability of the two conformations and/or the transition rate). Furthermore, the high frequency cluster also contains residues 64 and 66 of the bc loop of domain II, a mediator of the interaction between two E1 trimers in the so called "contact 2" region described in the E1-E1 interactions of the fusion protein of Semliki Forest virus(Gibbons et al., 2004). In particular, contact 2 involves interactions of residues 63-69 of the bc loop of one of the E1 trimers with residues 89–92 (part of the fusion loop) of the neighboring trimer. Residue 80 is at the core of the cluster, and the V80I mutation could affect the contact 2 region of the E1 trimer interface, which is known to be important in the early step of membrane fusion. **The A129V mutation,** alanine 129 is at the interface between domains I and II of E1, a major hinge region, controlling the inter-domain motion and the relative positioning of the domains in the protein. The alanine-to-valine mutation could therefore affect the internal conformation of E1 as well as conformational changes. Position 129 is also close to a main hinge in the dynamics of the E1-E2 dimer and the mutation could affect the flexibility and functional dynamics of the protein complex. Analysis of the slowest modes of motion of the E1 trimer structure (PDB ID: 1RER), corresponding to the low pH, fusion prone, conformation of the protein, shows that position 129 is a

hinge and position 80 is near a hinge (data not shown). This is further evidence for the importance of these positions for the dynamics and conformational changes.

Figure S4, related to Figure 5. Schematic of V80I:A129V:A226V emergence during transmission. The relative frequencies of the V80I:A129V mutations during infection and transmission suggest that the variants are first generated at low frequency in the tissues of the mosquito (body, mosquito 1), and accumulate to approximately 10-fold higher frequencies than in the original virus stock (indicated by star). The similar fitness of these variants compared to wild type in most tissues could account for the lack of substantially rapid selection within mosquito tissue itself. The first significant increase in frequency occurs in the cell-free saliva, where the variants are deposited and accumulate by maintaining structural integrity and infectivity with respect to the original parental strain (saliva, mosquito 1). The presence of these variants is maintained during passage in mammals (blood, mouse), although the increase or decrease in frequency appears to be stochastic and may depend on founder effects of which genotypes are first to replicate within the mammal. When present in mammals, transmission to mosquitoes results in a significant amplification of these variants in mosquito tissue, possibly aided by improved fusogenic activity (body, mosquito 2), followed by further amplification in saliva, where the V80I:A129V mutations become fixed to the majority genotype.

Figure S5, related to Figure 5. Emergence and transmission of V80I:A129V mutations in Asian mosquitoes. Mosquitoes were presented blood meals containing chikungunya A226V virus (d0) and infection was allowed to proceed for 10 days (d10). Individual mosquitoes were then separated and allowed to feed on individual

naïve mice, after which their saliva and bodies were harvested for deep sequencing. Mice exposed to infected mosquitoes were incubated for 5 days (d15), upon which time new batches of several mosquitoes were allowed to feed on individual mice. Mouse blood was then harvested for deep sequencing. The infection of the second set of mosquitoes was incubated for another 10 days (d25), at which points their bodies and saliva were harvested for deep sequencing. Deep sequence analysis of individual mosquito body, saliva and mouse blood samples are shown and represented in oval diagrams. The numbers indicate the percentage of the V80I:A129V mutations in each virus subpopulation. The background limit of detection was <0.01%, light shading represents >0.2%, medium shading >1.0% and dark shading >50%. ND, virus confirmed present, but not determined due to inability to obtain suitable amplicons for deep sequencing.

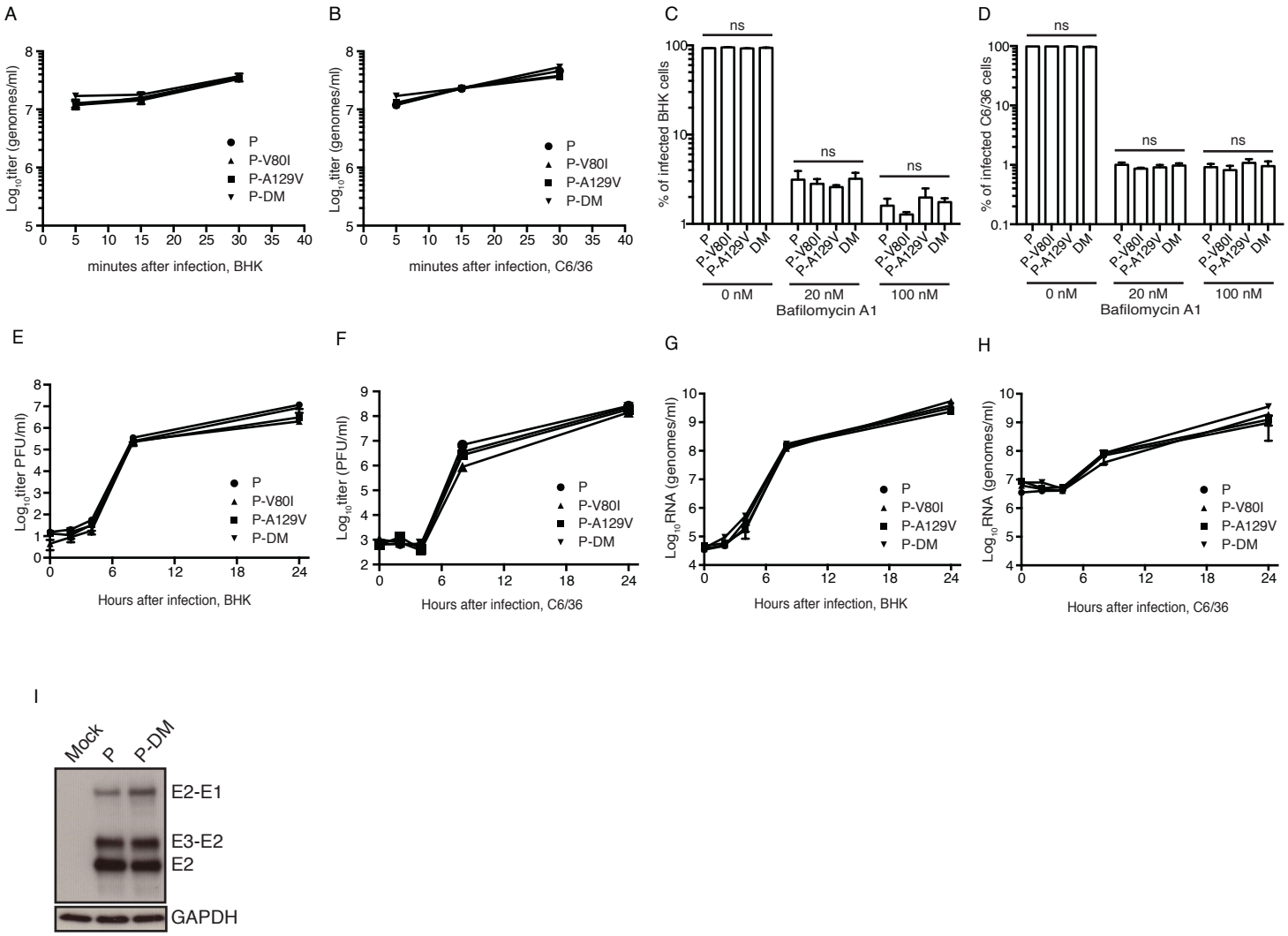
A
B
C
D
E
F
G
H
I
Log10titer (genomes/ml)
minutes after infection, BHK
minutes after infection, C6/36
P
P-V80I
P-A129V
P-DM
% of infected BHK cells
% of infected C6/36 cells
ns
0 nM
20 nM
100 nM
Bafilomycin A1
Log10titer PFU/ml)
Log10titer (PFU/ml)
Hours after infection, BHK
Hours after infection, C6/36
Log10RNA (genomes/ml)
Mock
E2-E1
E3-E2
E2
GAPDH

A

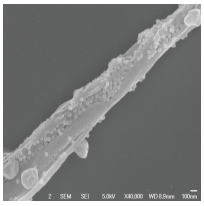

B

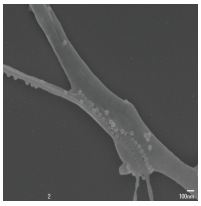

C

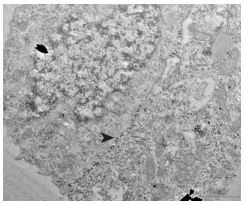

D

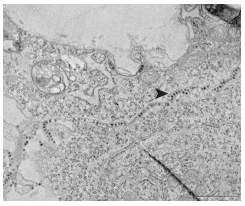

E

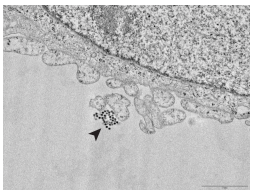

F

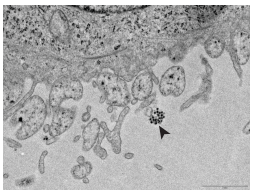

G

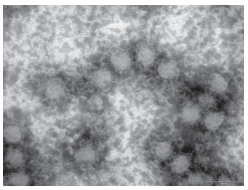

H

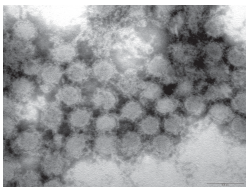

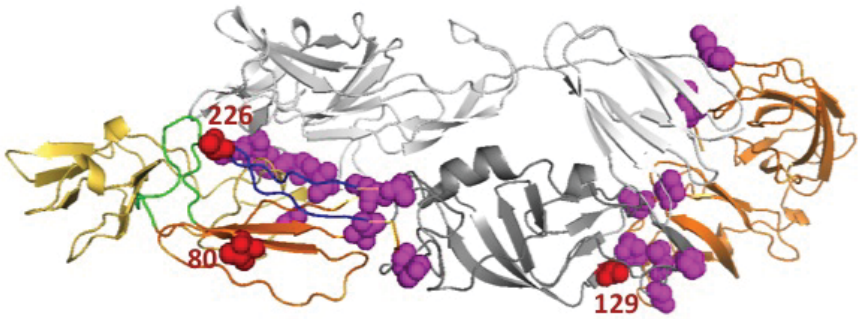
226
80
129

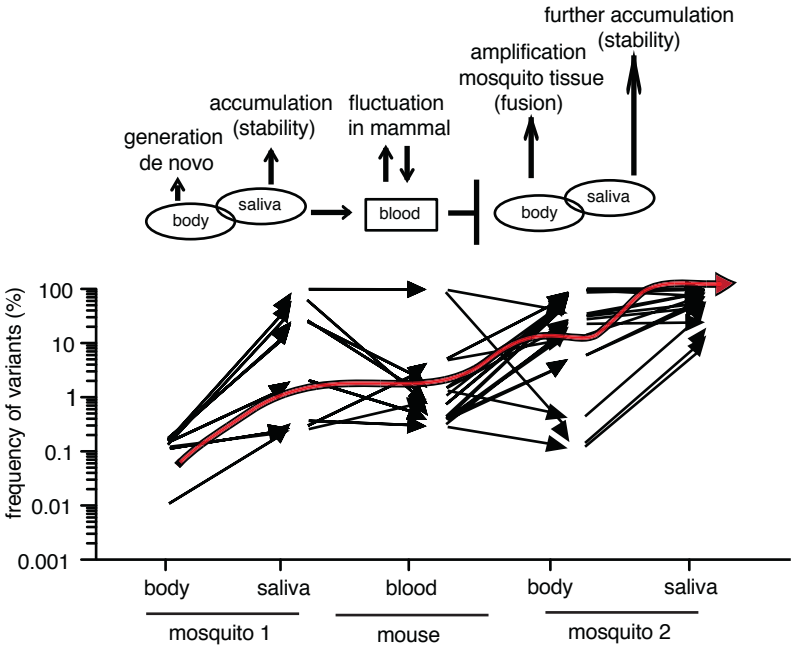
further accumulation
(stability)
amplification
mosquito tissue
(fusion)
accumulation
(stability)
fluctuation
in mammal
generation
de novo
body
saliva
blood
body
saliva
frequency of variants (%)
100
10
1
0.1
0.01
0.001
body
saliva
blood
body
saliva
mosquito 1
mouse
mosquito 2

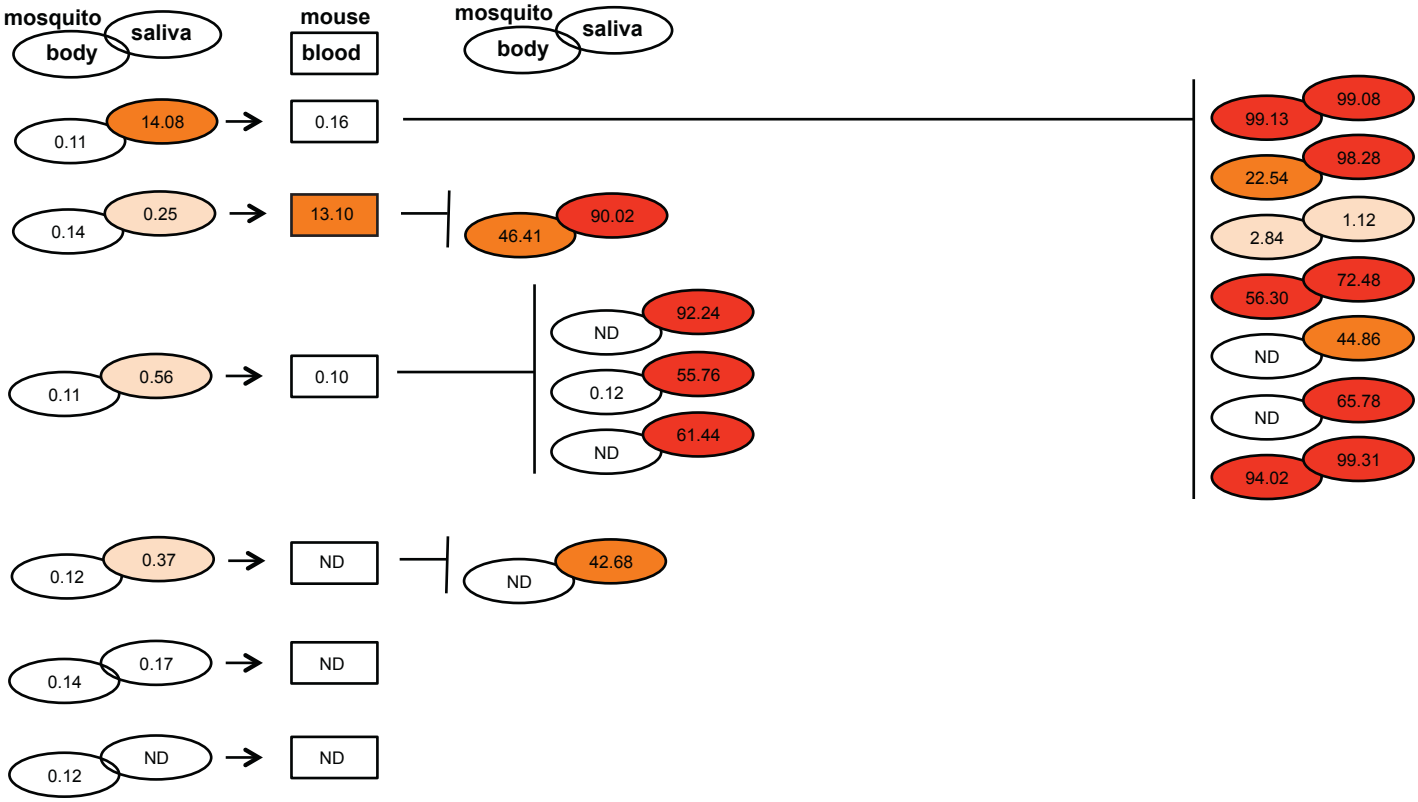
mosquito
body
saliva
mouse
blood
mosquito
body
saliva
0.11
14.08
0.16
99.13
99.08
22.54
98.28
2.84
1.12
56.30
72.48
ND
44.86
ND
65.78
94.02
99.31
0.14
0.25
13.10
46.41
90.02
0.11
0.56
0.10
ND
92.24
0.12
55.76
ND
61.44
0.12
0.37
ND
ND
42.68
0.14
0.17
ND
0.12
ND
ND

Experimental Procedures

Cells

Mammalian (BHK-21, Vero and HeLa) cells were maintained in GlutaMAX^{TM} Dulbecco's Modified Eagle Medium (DMEM) supplemented with 10% new-born calf serum (NCS) (Gibco) and 1% penicillin and streptomycin (P/S) (Sigma-Aldrich) at 37ºC with 5% CO_2. HEK293T, NIH3T3, Nor-10, A549, and BEAS-2B cells were maintained in DMEM supplemented with 10% fetal-bovine serum (FBS) and 1% P/S. *Aedes albopictus* cells (C6/36 and U4.4) and *Aedes aegypti* cells (Aag-2) were maintained in L-15 Leibovitz medium supplemented with 10% FBS, 1% tryptose phosphate broth, 1% nonessential amino acids, and 1% P/S at 28ºC. All cells were obtained from ATCC and confirmed free of mycoplasma.

Viruses

The infectious clone(Coffey and Vignuzzi, 2011) used to generate virus stocks in this study corresponds to chikungunya virus strain 06-049 (AM258994). To generate an isogenic chikungunya GFP-expressing infectious clone, the AgeI/XhoI restriction fragment of a previously purchased GFP-expressing infectious clone derived from chikungunya virus LR2006 (European Virus Archive) was inserted into the same restriction sites of the infectious clone described above. The 2012 Cambodian patient isolate was obtained after inoculation of a patient serum into C6/36 cells. The patient's blood sample was collected for diagnostic purposes by the National Centre for Malariology, Ministry of Health in Cambodia, during an outbreak investigation (which does not require prior approval from National Ethics Committee). The patient's sample and the virus strain were then anonymized for the purpose of this study. Both stocks contain the A226V mutation that emerged during the 2005/2006 Indian Ocean outbreak. The newly identified E1 mutations, V80I and A129V, were

introduced into the A226V infectious clone backbones using Quikchange II XL site-directed mutagenesis (Agilent) following the manufacturer's instructions. To study the pre-2005/2006 epidemic strain, residue 226V was reverted to the original A226 in a separate construct. The following primers were used to generate each mutation (in bold): V80I Forward 5' CCTGACTACAGCTGTAAG**A**TCTTCACCGGCGTCTACCC 3', V80IReverse 5' GGGTAGACGCCGGTGAAGA**T**CTTACAGCTGTAGTCAGG 3', A129V Forward 5' CAGGGCTCATACCGCATCTG**T**ATCAGCTAAGCTCCGCGTC 3', and A129V Reverse 5' GACGCGGAGCTTAGCTGAT**A**CAGATGCGGTATGAGCCCTG 3', V226AForward 5' CTGCAGAGACCGGCTG**C**GGGTACGGTACACGTG 3', and V226AReverse 5' CACGTGTACCGTACCC**G**CAGCCGGTCTCTGCAG 3'. 10 µg of each plasmid was linearized overnight with *NotI* followed by two phenol:chloroform extractions and an ethanol precipitation. Plasmids were resuspended in nuclease-free water at 1 µg/µl. *In vitro* transcribed viral RNAs were produced from linearized plasmids using the SP6 mMESSAGE mMACHINE kit (Ambion) following the manufacturer's instructions. After RNA synthesis, samples were DNase treated and RNAs were purified by phenol:chloroform extraction, ethanol precipitation, and resuspended at a concentration of 1 µg/µl. All RNAs were stored at -80ºC until electroporation. Infectious virus was produced by electroporating BHK cells with *in vitro* transcribed viral RNAs. BHK cells were trypsinized, washed twice with ice-cold PBS, and resuspended at $2x10^7$ cells/ml in PBS. 390 µl of cells were mixed with 10 µl (10 µg) of *in vitro* transcribed RNA and added to a 2 mm electroporation cuvette. Cells were electroporated with 2 pulses at 1.2 kV, 25 F, with infinite resistance in a XCell Gene Pulser (BioRad). Cells were allowed to recover for 10 min at room temperature, transferred into 6 ml of warm DMEM, and placed in a T25 flask at 37ºC for 48 h. Virus was harvested, spun at 1,200 x g for 5 min to remove debris, and viral titers were determined by plaque assay.

Virus titrations

For plaque assays, 10-fold serial dilutions of virus were made in DMEM and each dilution was incubated on a Vero monolayer for 1 h. Following incubations, a 0.8% agarose overlay was added containing DMEM with 2% NCS, and plaques were allowed to develop for 72 h. Cells and virus were then fixed with 4% formalin, the agarose plugs were removed, and plaques were visualized by staining with crystal violet (10% crystal violet with 20% ethanol in H_2O). Titers were recorded as the reciprocal of the highest dilution where plaques were noted. The limit of detection was 2.9 log10 PFU/ml.

Viral RNA extractions and qRT-PCR

Viral RNA was isolated using TRIzol (Sigma-Aldrich) following manufacturer's instructions. Viral RNA concentrations were measured with qRT-PCR using the Taqman RNA-to-C_T one-step quantitative RT-PCR kit (Applied Biosystems) as previously described(Coffey and Vignuzzi, 2011). A standard curve was generated for each data set from duplicate replicates of *in vitro* transcribed RNAs.

Virus binding assays

BHK and C6/36 cells were incubated with CHIKV (MOI=5) at 4°C for the indicated times. At each time point, virus inoculum was removed, cells were washed three times with ice-cold PBS, and 500 µl of TRIzol was added for viral RNA extractions and qRT-PCR.

Lysosomotropic agent treatment

BHK and C6/36 cells were pre-incubated in media containing 0, 20 or 100 nM of Bafilomycin A1 for 1 h. Virus was diluted to an MOI of 5 in DMEM containing each inhibitor and added to cells for 1 h. Cells were washed extensively with PBS and media containing Bafilomycin A1 was added for 16 h. Following treatment, supernatants were removed, cells washed with PBS, trypsinized, and fixed in 1% paraformaldehyde (PFA). The number of GFP-expressing cells was quantified by flow cytometry.

Fusion from without assay

BHK and MEF cells were chilled at 4°C and pre-incubated in binding buffer (RPMI, 10 mM HEPES, 2% bovine serum albumin (BSA), 20 mM NH_4Cl, pH 7.4) for 1 h. Each virus was diluted in binding buffer and added to cells at an MOI of 5 for 1 h at 4°C. Unbound virus was removed and viral fusion was induced by the addition of pre-warmed fusion buffer (RPMI, 10 mM HEPES, 2% BSA) adjusted to each pH described for 2 min at 37°C. The pH was neutralized by the addition of complete media containing 20 mM NH_4Cl and fusion was analyzed by flow cytometry.

Virus "pre-triggering" assay

To address the role of pH prior to membrane binding, GFP-expressing viruses were preincubated in fusion buffer (RPMI, 10 mM HEPES, 2% BSA) adjusted to the indicated pH for 1 h at 37ºC. The pH was neutralized by the addition DMEM and viral infectivity was measured by flow cytometry.

Growth curves and RNA synthesis

One-step viral growth curves were performed in triplicate by infecting BHK and C6/36 cells with each virus variant at an MOI = 1 for 1 h. Cells were washed 3 times with 1X PBS to remove unbound virus and fresh media was added. Supernatant aliquots were taken at each time point and an equal volume of fresh media was added back to compensate for removed volume. U4.4 and Aag2 cells were infected at MOI = 10 and progeny virus was tittered from supernatant 24 h after infection. HEK293T, NIH3T3, Nor-10, A549, and BEAS-2B cells were infected at an MOI = 1 and progeny virus was titrated from supernatants 24 h after infection. Viral titers were determined by plaque assay. To determine rate of RNA synthesis, viral RNA was extracted from supernatants and quantified by qRT-PCR.

Virion stability

Virus stocks were diluted to 10^5 PFU/ml in culture medium and incubated at 28ºC or 37ºC. At 0, 8, 24 and 48 hours, 100 µl aliquots were taken for titration of infectivity by plaque assay

and for quantification of virus particles containing genomes by qRT-PCR. The specific infectivity was determined by dividing the infectious virus PFU values by the total number of genomes contained in the viral particles. At time zero, all virus stocks presented similar infectious titers and specific infectivities (between 0.203 and 0.217).

Fusion-blocking antibody dynamics

Antibodies CHIK102, 152, 166, 263 were a kind gift from Michael Diamond(Pal et al., 2013). To address virus fusion in the presence of blocking antibodies, ~50 PFU of each virus were incubated at 4ºC on a monolayer of Vero cells for 1 h. Cells were washed extensively with ice-cold PBS and blocking antibodies, diluted in DMEM, were added to cells for 1 h at 4ºC. To induce virus fusion, cells were incubated at 37ºC for 15 min followed by the addition of an agarose overlay. Antibody inhibition was addressed 72 hours later.

Virion purification

Viral particles were pelleted by ultracentrifugation at 25,000 x g for 2 hours at 4°C through a 20% sucrose cushion. The pellet was resuspended in sterile filtered PBS and passed three times through a 100K Ambion centrifugal filter column (Millipore) and resuspended in sterile filter PBS.

Electron Microscopy

For scanning electron microscopy HeLa and C6/36 cells were fixed in 2.5% glutaraldehyde in 0.1 M cacodylate buffer (pH 7.2), washed in 0.2 M cacodylate buffer (pH 7.2), postfixed for 1 h in 1% osmium tetroxide in 0.1 M cacodylate buffer (pH 7.2), and then rinsed with distilled water. Samples were dehydrated through a graded series of 25, 50, 75, 95 and 100% ethanol solution followed by critical point drying with CO_2. Dried specimens were sputtered with 10 nm gold palladium, with a GATAN Ion Beam Coater and were examined and photographed with a JEOL JSM 6700F field emission scanning electron microscope operating at 5 Kv. Images were acquired with the upper SE detector (SEI) .

For transmission electron microscopy, cells were fixed overnight at 4°C with 2,5% glutaraldehyde in 0.1M cacodylate buffer, pH 7.4, and postfixed in 1% osmium tetroxide in 0.1 M cacodylate buffer, pH 7.4, for 1 h. After being rinsed in 0.1M cacodylate buffer, cells were transferred to 0.2M cacodylate buffer for 30 min. Cells were washed in 30% methanol for 10 min, stained in 2% uranyl acetate-30% methanol for 1h, and washed in 30% methanol. Cells were then dehydrated in an ethanol series and embedded in Epon. Thin sections were cut with a Leica Ultramicrotome Reichert Ultracut S, stained with uranyl acetate. Purified viral particles were fixed with 2.5% gluteraldehyde in 0.1M cacodylate buffer, pH 7.4, washed twice with sterile filtered H_2O, and stained with 1% phosphotungstic acid (PTA). Images were taken with a JEOL 1200EX2 Electron Microscope at 80kV equipped with an Eloïse Keen View camera.

Immunoblotting

BHK cells were infected at an MOI=1 and incubated for 24 hours. Cells were harvested, washed with PBS, and resuspended in 2x SDS-PAGE buffer containing 5% beta-mercaptoethanol (BioRad). Proteins were separated on a 4-20% TGX-Miniprotean gel (BioRad), transferred to a nitrocellulose membrane, blocked in 5% non-fat milk in phosphate buffer saline containing 0.1% Tween-20 (PBST), and incubated with primary anti-mouse chikungunya virus E2 antibody (CHIK48 – a kind gift from Michael Diamond). Membranes were washed extensively and incubated with ECL anti-mouse IgG horseradish peroxidise (HRP) secondary antibody (GE Healthcare), and developed with SuperSignal West Pico chemiluminescent substrate (Pierce).

Normal mode analysis

Normal mode analysis of E1 and the E1/E2 dimer were conducted using the Gaussian Network Model (GNM)(Emekli et al., 2008; Haliloglu et al., 1997) and the X-ray crystal structure of chikungunya virus particles E1-E2 (PDB code: 2XFB)(Voss et al., 2010), where

E1 is in complex with E2. GNM describes the protein structure as elastic network, in which the α-carbon atoms within a cut-off radius are assumed to be connected by Hookean springs, displaying Gausssian fluctuations around their mean positions. The correlation between two nodes i and j, $\Delta\mathbf{R}_i$ and $\Delta\mathbf{R}_j$, respectively, are calculated as $<\Delta\mathbf{R}_i\Delta\mathbf{R}_j> = (3k_BT/\gamma)[\boldsymbol{\Gamma}^{-1}]_{ij} = (3k_BT/\gamma)\sum_k[\lambda_k^{-1}\mathbf{u}_k\mathbf{u}_k^T]_{ij}$

where $\boldsymbol{\Gamma}$ is an $N \times N$ Kirchhoff matrix of the inter-node contacts with the (commonly used) cutoff of 10 Å, where N is the number of amino acids in the protein. $\mathbf{u}_k$ and λ_k are the k-th eigenvectors and eigenvalues of $\boldsymbol{\Gamma}$, k_B is the Boltzmann constant, T is the absolute temperature, and γ is a uniform force constant; k_BT/γ was taken as 1 Å^2. Overall, Eq. 1 predicts the mean-square displacement of each residue when $i = j$ and the correlations between the fluctuations of residues i and j when $i \neq j$, and when $i \neq j$, it predicts the correlations between the fluctuations of residues i and j as a superimposition of N-1 eigenmodes from the slowest to fastest modes of motion. Slow modes refer to cooperative and global motions, whereas fast modes refer to the residues displaying localized fast fluctuations. The results of the analysis of E1 alone are presented in Fig. 4B and of the E1/E2 complex in Supplemented Fig. S3.

Mosquito infections and harvests

Aedes aegypti (1 lab-reared Rockefeller colony, 1 colony, F10 generation, collected in Bénoué, Cameroon in September 2007; 1 colony, F2 generations collected in Nakhon Chum, Thailand in 2011; 1 colony, F3 generations, collected in Kampong Cham, Cambodia) and *Aedes albopictus* (1 colony, F14 generation, collected in Bertoua, Cameroon in September 2007; 1 colony, F2 generations, collected in Phu Hoa, Vietnam in 2011) were used for mosquito infections. Viruses were diluted to 10^3 or 10^5 PFU/ml and mixed 1:2 with pre-washed rabbit blood. Female mosquitoes were allowed to feed on 37ºC blood meals through a chicken skin membrane for 20-60 min after which engorged females were incubated at 28ºC with 10% sucrose *ad libitum*, females that did not feed were excluded. Matched titers of

blood meals (within 0.3 $\log_{10}$ PFU/ml) were verified by titrations of blood meals immediately after feeds. After incubations, legs and wings were removed, the proboscis of each mosquito was inserted into a capillary tube containing 5 µl FBS for 45 m. Midguts, legs/wings and salivary glands were dissected in PBS under 10X magnification. Saliva samples in FBS were added to 45 µl of L-15 media and the legs/wings, bodies and salivary glands were placed in 2 ml round bottom tubes containing 300 µl DMEM and a steel ball. Samples were ground in a MM300 homogenizer (Retsch) at 30 shakes/s for 2 min. For infectivity determinations, whole bodies were ground individually, using the same homogenization methods. At least 20 mosquitoes were used per sample to ensure that enough mosquitoes fed and became positively infected for downstream analysis.

Mouse infections

Mice were kept in the Pasteur Institute animal facilities in BSL-3 isolators, with water and food supplied *ad libitum*, and handled in accordance with institutional guidelines for animal welfare and at endpoint, were humanely euthanized complying with the Animal Committee regulations of Institut Pasteur in Paris, France, in accordance with the EC 86/609/CEE directive. 8-day old C57B/6 mice were injected subcutaneously in the back with 200 PFU of virus and at selected times post-inoculation, animals were sacrificed and blood and organs were harvested. Organs were placed individually in tubes and homogenized as for mosquitoes. Survival curves were generated by injecting 8-day or 3-week old female mice with 10^6 PFU of virus and monitoring morbidity and mortality for 14 d after infection.

Transmission studies

Transmission experiments were conducted at the Institut Pasteur in Cambodia in Phnom Penh in BSL3 facilities. Briefly, mosquitoes were infected as described previously and incubated at 28°C for ten days. On day ten, individual mosquitoes were allowed to feed on individual five day old Swiss mice until engorged. 5-day old Swiss mice were immobilized on a mesh

surface suspended over a cup containing an individual mosquito at 28ºC. Mice and mosquitoes were incubated together for 1 hour or until feeding had occurred. Following feeding mice were returned to cages and individual mosquitoes were salivated and their bodies crushed and harvested. Mice were monitored for disease for five days. After five days of infection in mice, naïve mosquitoes were allowed to feed on individual infected mice until engorged. Following feeding, mice were sacrificed and blood was harvested. These mosquitoes were then incubated at 28°C for ten days, salivated and their bodies crushed and harvested. Amplicons for deep sequencing were prepared immediately after harvesting *in vivo* samples, which improved the overall yield compared to using frozen samples.

High-throughput Sanger sequencing and genetic diversity

For genetic diversity and bottleneck experiments, amplicons flanking the partial E1 gene were generated using the Titan one-step RT-PCR kit (Roche) and primers flanking genome positions 9943–10746. Amplicons were cloned into TOPO vectors (Invitrogen) and sequenced using Sanger technology in 96-well format (GATC Biotech). Mutation frequencies were determined by dividing the number of nucleotide polymorphisms in all clones (where polymorphisms at the same genetic locus on multiple clones were counted once) by the number of nucleotides sequenced. Values were then represented as number of mutations per 104 nt sequenced. Each frequency was corrected by subtracting the background mutation frequency, defined as the mutation frequency in TOPO-cloned clone plasmid DNA sequences. In vitro transcribed clone RNA subjected to the same RT-PCR and TOPO cloning demonstrated a mutation frequency that was not significantly different from cloned plasmid (data not shown), indicating that the RT-PCR was not a significant source of mutational error.

Deep sequencing of samples

Viral RNAs were isolated from samples by Trizol extraction, and the E1 gene was amplified using the Titan one-step RT-PCR kit (Roche) with the following primers: E1Forward(9943)

5′ TACGAACACGTAACAGTGATCC 3′ and E1Reverse(10726) 5′ CGCTCTTACCGGGTTTGTTG 3′ following manufacturer's instructions. PCR fragments were purified via the Nucleospin Gel and PCR Clean-up kit (Macherey-Nagel) and total DNA was quantified by Nano-drop. PCR products were then fragmented (Fragmentase), linked to Illumina multiplex adapters, clusterized and sequenced with Illumina cBot and GAIIX technology. Sequences were demultiplexed using Illumina's CASAVA software, allowing for no mismatches in the multiplex tag sequences. Quality filtering (95-98% of reads passed) and adaptor cleaning was done using fastq-clipper (http://hannonlab.cshl.edu/fastx_toolkit/index.html). The 75-nt reads were aligned to the E1 sequence as a reference, with a maximum 2 mismatches per read, using BWA(Li and Durbin, 2009). Alignments were processed using SAMTOOLS(Li et al., 2009) to obtain the nucleotide/base calling at each position. An in-house ViVAn (Virus Variance Analysis) pipeline was used to identify statistically significant variants above the background noise due to sequencing error, calculated for each nucleotide site. Briefly, for each position throughout the viral genome, base identity and their quality scores were gathered. Each variant allele's rate was initially modified according to its covering read qualities based on a maximum likelihood estimation, and tested for significance using a generalized likelihood-ratio test. Additionally, an allele confidence interval was calculated for each allele. In order to correct for multiple testing, Benjamini-Hochberg false-discovery rate of 5% was set. In all experiments, a minimum coverage of 25,000 reads was obtained and the background error at every nucleotide site was always below 0.01%.

Statistical Analyses

No samples or infected animals were excluded from analysis. Animals were randomly allocated to groups before infections were performed. No blinding was performed during experimentation and analysis. All statistical tests (described in each figure legend) were

conducted using GraphPad Prism software. P-values >0.05 were considered non-significant (ns).

Coffey, L.L., and Vignuzzi, M. (2011). Host alternation of chikungunya virus increases fitness while restricting population diversity and adaptability to novel selective pressures. J. Virol. *85*, 1025–1035.

Emekli, U., Schneidman-Duhovny, D., Wolfson, H.J., Nussinov, R., and Haliloglu, T. (2008). HingeProt: automated prediction of hinges in protein structures. Proteins *70*, 1219–1227.

Haliloglu, T., Bahar, I., and Erman, B. (1997). Gaussian dynamics of folded proteins. Physical Review Letters.

Li, H., and Durbin, R. (2009). Fast and accurate short read alignment with Burrows-Wheeler transform. Bioinformatics *25*, 1754–1760.

Li, H., Handsaker, B., Wysoker, A., Fennell, T., Ruan, J., Homer, N., Marth, G., Abecasis, G., Durbin, R., and Subgroup, 1.G.P.D.P. (2009). The Sequence Alignment/Map format and SAMtools. Bioinformatics *25*, 2078–2079.

Pal, P., Dowd, K.A., Brien, J.D., Edeling, M.A., Gorlatov, S., Johnson, S., Lee, I., Akahata, W., Nabel, G.J., Richter, M.K.S., et al. (2013). Development of a highly protective combination monoclonal antibody therapy against Chikungunya virus. PLOS Pathogens *9*, e1003312.

Voss, J.E., Vaney, M.-C., Duquerroy, S., Vonrhein, C., Girard-Blanc, C., Crublet, E., Thompson, A., Bricogne, G., and Rey, F.A. (2010). Glycoprotein organization of Chikungunya virus particles revealed by X-ray crystallography. Nature *468*, 709–712.